

Parametric study of reinforced earth wall deformations

Etude paramétrique des déformations d'un mur de sol armé

B. Stanić

Civil Engineering Institute of Croatia, Zagreb, Croatia

M.S. Kovačević & A. Szavits-Nossan

Faculty of Civil Engineering, University of Zagreb, Croatia

ABSTRACT

The paper presents results of an extensive parametric study on deformations and internal forces developing in reinforced soil walls consisting of gabion basket facing units keyed into the backfill of crushed rocks by wire meshes. The parameters studied covered the wall geometry and the mechanical characteristics of wall elements. Deformations and internal forces were obtained by numerical modelling with material parameters determined from field measurements on constructed walls.

RÉSUMÉ

Les résultats sont présentés d'une étude paramétrique extensive des déformations et des forces internes qui se développent dans un mur de sol armé. Le mur armé est composé des gabions à sa face, et les gabions sont serrés à la pierre écrasée derrière le mur par des mailles de fil de fer. Parmi les paramètres étudiés sont la géométrie du mur et les caractéristiques mécaniques des éléments du mur. Les déformations et les forces internes ont été calculées par la modélisation numérique en utilisant les paramètres des matériaux déduits des mesures sur les murs qui ont été déjà construits.

1 INTRODUCTION

Reinforced earth walls are gaining popularity in Croatia, particularly after several were successfully constructed in large motorway projects. For these walls, the Maccaferri Terramesh System, consisting of gabion basket facing units keyed into the backfill of crushed rocks by hexagonal double twisted wire meshes, was used. Several of them were extensively monitored during and after construction by measuring the wire mesh elongations. This was performed using sliding deformer casings (Kovári & Amstad, 1982) clamped to the mesh (Stanić et al., 2001). The small strain rockfill stiffness was measured in situ by SASW. It became immediately apparent that measured deformations did not correspond well with deformations estimated from forces calculated by the classical limit equilibrium methods. In order to improve the understanding of the wall behaviour, sophisticated analyses by numerical modelling were undertaken. Using published data on the strain dependent mesh stiffness and estimated strain dependent stiffness of the rockfill, adjusted to measured values at small strains, it was possible to obtain good correlations between measured mesh deformations and deformations obtained by numerical modelling (Stanić, 2002; Stanić et al., 2003). Numerical analyses were performed by using the FLAC program with specially developed original nonlinear constitutive equations for the mesh and the rockfill.

In order to gain further insight into the behaviour of reinforced walls, an extensive parametric study, using numerical modelling, was undertaken by varying the main wall parameters.

2 THE PARAMETRIC STUDY

2.1 The structural model of the reinforced earth wall

Stresses and deformations in reinforced earth walls (Fig. 1) were calculated using the FLAC program. Actual construction sequences, consisting of placing successive layers of rockfill

and reinforcements on the ground level, were closely simulated. The foundation soil/rock was assumed elastic, characterized by a shear modulus and Poisson ratio, as indicated in Figure 1. The rockfill behaviour was described by a kinematic hardening, elasto-plastic model incorporating the Mohr-Coulomb failure criterion with a friction angle φ without cohesion and dilatancy (Szavits-Nossan & Kovačević, 1994; Szavits-Nossan et al., 1999).

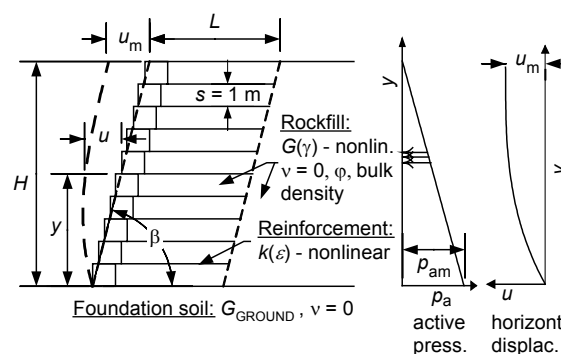


Figure 1. Cross section through the reinforced earth wall: geometry, materials, displacements, and notations

In monotonic shear the model response is represented by a tri-linear stress-strain relationship extending from very small shear strains up to large shear strains at failure. At very small strains the material response is elastic with a constant shear modulus G_0 and a Poisson ratio $\nu = 0$. At larger strains the shear modulus G decays as shear strength τ_f is approached. As no data on shear modulus decay for rockfill were available, this parameter was adjusted to match published data on sands. The shear modulus decay can be normalized for monotonic shear, as shown in Figure 2. The secant shear modulus G is normalized by the elastic shear modulus at very small strains, G_0 , while the shear strain γ is normalized by the elastic shear strain at failure $\gamma_r = \tau_f/G_0$. Under monotonic hydrostatic loading, the model behaves as linear elastic.

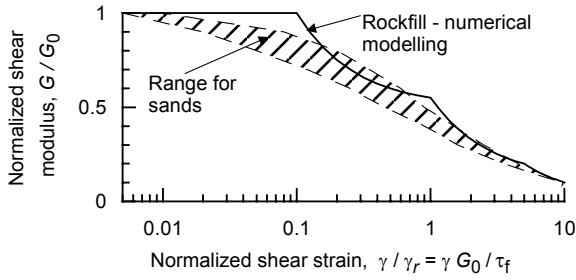


Figure 2. Shear modulus decay from very small strains up to failure used in numerical modelling of rockfill

The earth reinforcements were modelled by one-dimensional tension elements. Experiments by Lo (1990) on wire mesh deformations, with the mesh constrained by normal pressure σ , exerted perpendicular to the mesh surface by coarse backfill, were interpreted to give the following relation for its tensile stiffness per mesh width

$$k \text{ (MN/m)} = \begin{cases} k_0 & \text{for } 0.135\varepsilon^{-0.69} \geq k_0 \\ 0.135\varepsilon^{-0.69} & \text{for } 0.135\varepsilon^{-0.69} < k_0 \text{ and } \varepsilon \leq \varepsilon_f \\ 0.0 & \text{for } \varepsilon > \varepsilon_f \end{cases} \quad (1)$$

where k is the tensile stiffness of the mesh ($= T/\varepsilon$), T being the tensile force per mesh width in MN/m, ε is the linear tensile strain of the mesh, ε_f is the failure strain at which the mesh ruptures and loses its stiffness, and k_0 is the initial (elastic) mesh stiffness. The failure strain was found to depend on normal stress and equal to 2% for σ greater than 150 kPa, equal to 3% for σ between 75 kPa and 150 kPa, and equal to 4.5% for σ below 75 kPa. The initial stiffness k_0 was taken as 12 MN/m as the best fit from experimental data.

2.2 The reference wall, force and displacement

A 12 m high vertical wall with 8 m long reinforcements, constructed on stiff horizontal ground, was taken as the reference wall, that other walls with different geometry and material parameters were compared to. The material parameters of the reference wall were taken close to the values found appropriate in numerical analyses for the previously mentioned monitored walls. The initial shear modulus for the rockfill of the reference wall was taken as $G_0 = 40$ MPa, the rockfill friction angle as $\varphi = 40^\circ$, and the initial wire mesh stiffness as $k_0 = 12$ MN/m.

Among various aspects of the wall behaviour, two, probably most interesting, were selected for presentation: horizontal displacements of the wall face (u) versus normalized vertical distance from the wall base (y/H from Fig. 1), and the maximum

tensile force (T) developed in a reinforcement row, also versus the normalized vertical distance.

In order to ease the understanding of the complex wall behaviour, calculated horizontal wall displacements were normalized by the maximum horizontal displacement (u_m) of a vertical elastic shear beam of height H , width L and shear modulus G_0 , fixed at the ground level and horizontally loaded by the simple Rankine's triangular active earth pressure distribution p_a (Fig. 1). The vertical beam, horizontally loaded by the backfill, represents a very simplified model of the reinforced earth wall. The maximum lateral pressure on the beam is then given by the well-known expression

$$p_{am} = K_a \rho g H \quad (2)$$

where $K_a = \tan^2(45^\circ - \varphi/2)$ and represents the active pressure coefficient, ρ is the bulk density of rockfill (taken as 2 Mg/m^3 in this study), and g is the acceleration of gravity. A simple analysis gives the maximum horizontal displacement of the elastic shear beam (at the top of the beam) as

$$u_m \text{ el. shear beam} = \frac{K_a \rho g H^3}{6 L G_0} \quad (3)$$

Similarly, the maximum calculated tensile force in reinforcements (T) was normalized with the force T_a given as

$$T_a = p_{am} s \quad (4)$$

where s is the spacing between reinforcement rows. Force T_a is the tensile force in the lowest reinforcement row as given by the classical analysis of reinforced walls.

2.3 Results of the parametric study

The following Figures present various influences of reinforced wall parameters on calculated vertical distributions of normalized horizontal displacements of the wall face and normalized maximum tensile forces in reinforcement rows. Full lines represent results obtained by numerical modelling. Dashed lines in the left hand-side Figures represent horizontal displacements for the simple elastic shear beam, while in the right hand-side Figures they represent the distribution of tensile forces in reinforcements obtained from the classical reinforced earth model. Close inspection of these Figures reveals that the friction angle of the rockfill (Fig. 4), and the wall height with the constant width to height ratio (Fig. 8), have little influence on normalized horizontal displacements (u/u_m). The same may be concluded for the influence of the rockfill initial shear modulus (Fig. 5), the ground stiffness (Fig. 6) and the reinforcement length to the

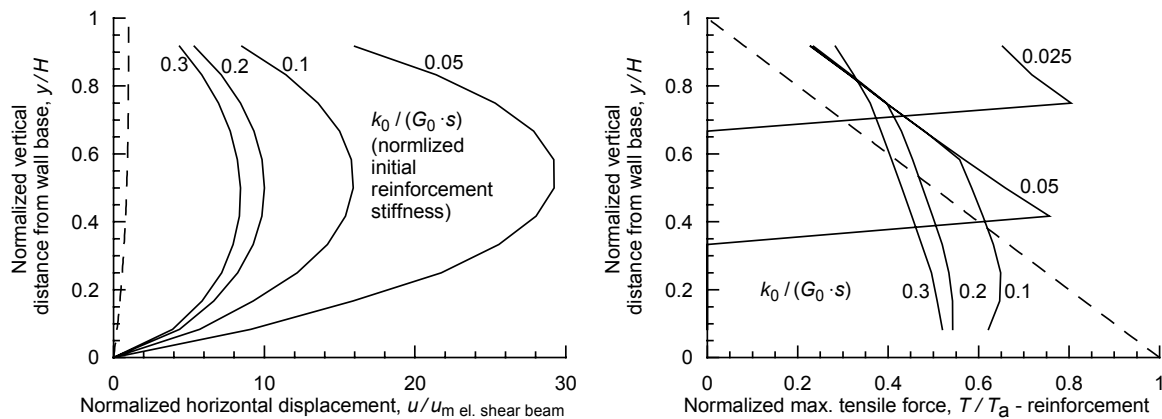


Figure 3. Influence of initial wire mesh stiffness k_0 ; ($H = 12$ m, $L = 8$ m, $\beta = 90^\circ$, $G_0 = 40$ MPa; $\varphi = 40^\circ$, $G_{\text{GROUND}} = \infty$)

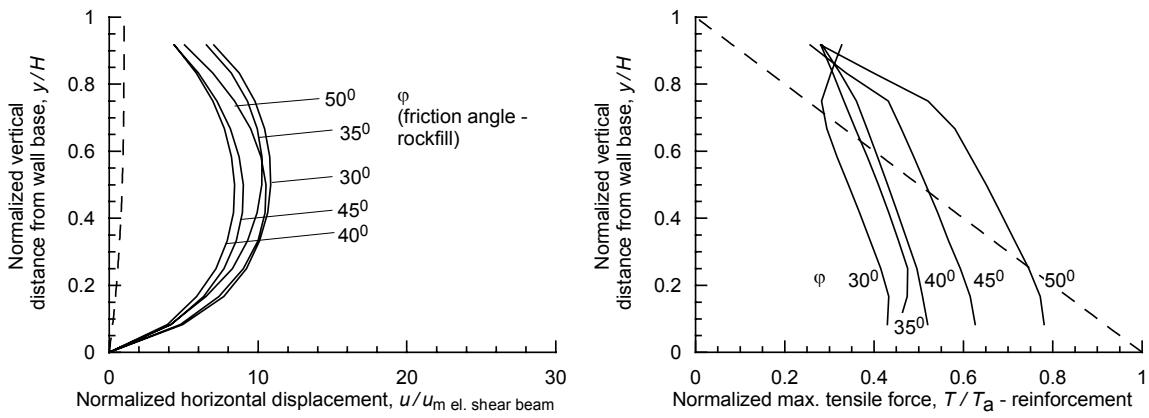


Figure 4. Influence of the friction angle for rockfill; ($H = 12 \text{ m}$, $L = 8 \text{ m}$, $\beta = 90^\circ$, $G_0 = 40 \text{ MPa}$; $k_0 = 12 \text{ MPa}$, $G_{\text{GROUND}} = \infty$)

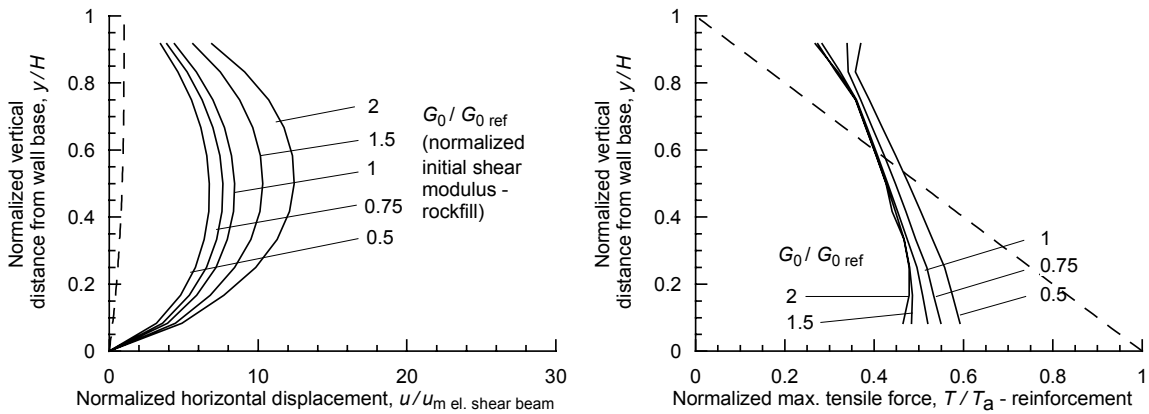


Figure 5. Influence of the initial shear modulus G_0 for rockfill; ($H = 12 \text{ m}$, $L = 8 \text{ m}$, $\beta = 90^\circ$, $G_{0 \text{ ref}} = 40 \text{ MPa}$, $\varphi = 40^\circ$; $k_0 = 12 \text{ MPa}$, $G_{\text{GROUND}} = \infty$)

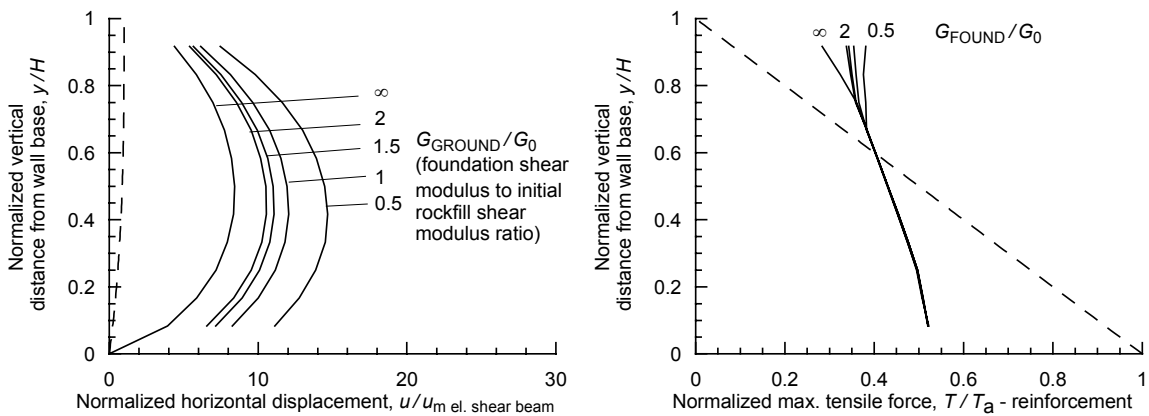


Figure 6. Influence of the shear modulus G_{GROUND} for the foundation soil/rock; ($H = 12 \text{ m}$, $L = 8 \text{ m}$, $\beta = 90^\circ$, $G_0 = 40 \text{ MPa}$, $\varphi = 40^\circ$; $k_0 = 12 \text{ MPa}$.)

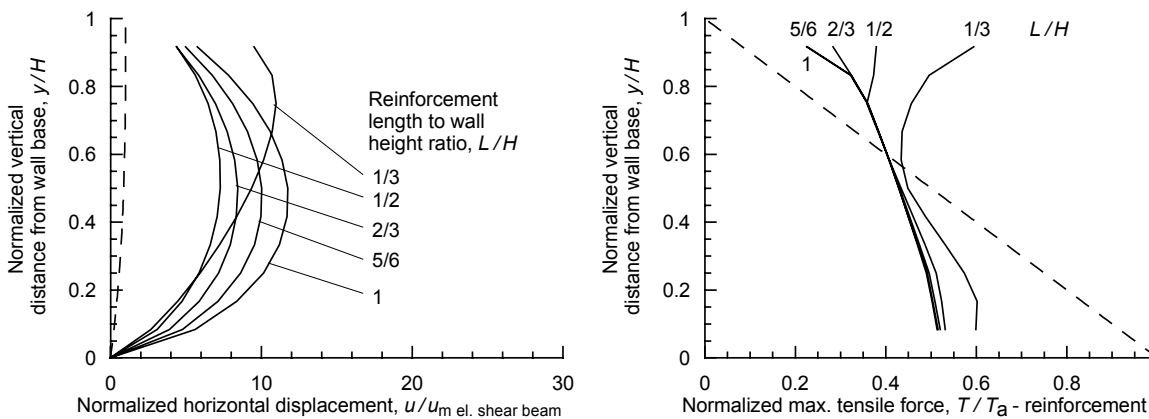


Figure 7. Influence of the reinforcement length to the wall height ratio; ($H = 12 \text{ m}$, $L = 8 \text{ m}$, $\beta = 90^\circ$, $G_0 = 40 \text{ MPa}$, $\varphi = 40^\circ$; $k_0 = 12 \text{ MPa}$, $G_{\text{GROUND}} = \infty$)

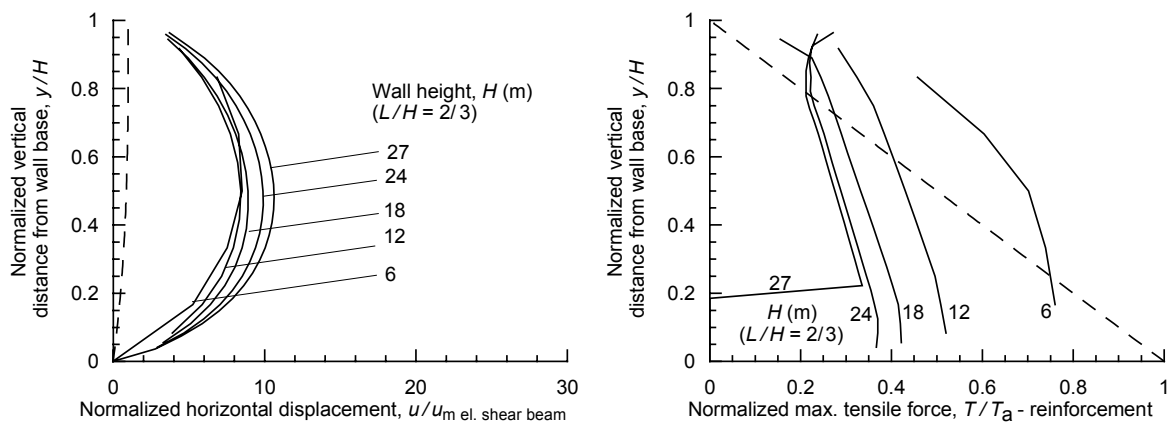


Figure 8. Influence of the wall height H ; ($L/H = 2/3$, $\beta = 90^\circ$, $G_0 = 40$ MPa, $\varphi = 40^\circ$; $k_0 = 12$ MPa, $G_{\text{GROUND}} = \infty$)

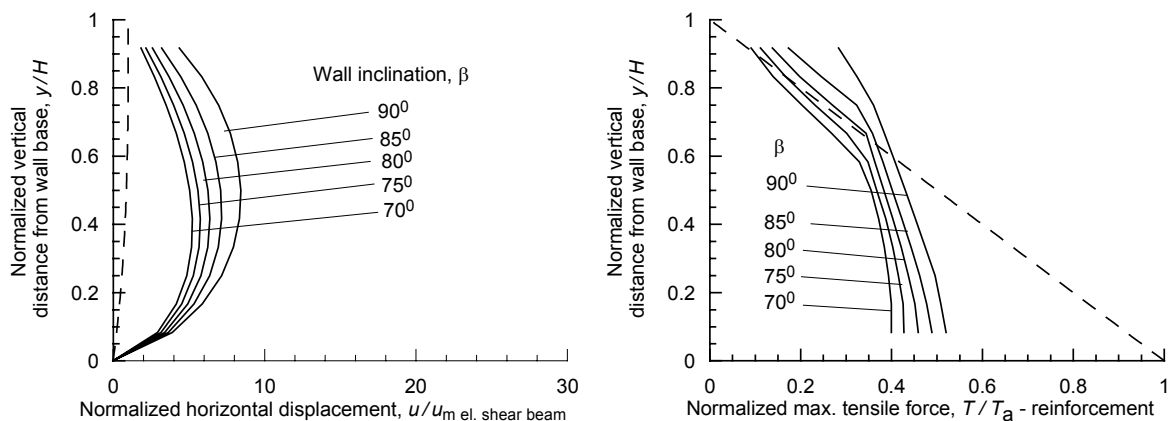


Figure 9. Influence of the wall inclination β ; ($H = 12$ m, $L = 8$ m, $G_0 = 40$ MPa, $\varphi = 40^\circ$; $k_0 = 12$ MPa, $G_{\text{GROUND}} = \infty$)

wall height ratio (Fig. 7), on the normalized maximum tensile force in reinforcements (T/T_a).

While the maximum normalized horizontal displacements for all considered cases are larger for roughly an order of magnitude, or more, than the corresponding values for the elastic shear beam, indicating that the shear beam is not an appropriate simplification for reinforced wall behaviour, the magnitudes of tension forces in reinforcements correspond in average to the values obtained by the classical reinforced earth model. It can be deduced from Figure 8 and with help of Equation (4) that the horizontal wall displacements increase with the square of the wall height for a constant width to height ratio. The maximum tensile force distribution generally shows that reinforcements in the upper part of the wall are more stressed than they would be according to the classical reinforced earth model, while the reverse holds for the reinforcements in the lower part of the wall. It can also be observed that the normalized tensile force in reinforcement rows is larger for low than for high walls with the same L/H ratio. The maximum tensile forces in reinforcements decrease as the wall face is more inclined (Fig. 9), as would be expected.

Of particular interest are the influences of the wall height and the reinforcement length to wall height ratio. Figure 8 infers that a 27 m high wall is on the brink of collapse, since the tensile forces in the lower five reinforcement rows have dropped to zero (due to simulated rupture of wire meshes). Probably 20 m is the upper safe limit for the height of vertical Terramesh System walls. On the other hand, Figure 7 reveals that for reinforcement length to wall height ratios of $1/2$ or less, reinforcements in the upper third of the wall become overstressed (although only the wall with $L/H = 1/3$ shows signs of collapse). This would not be predicted by the classical theory.

3 CONCLUSIONS

By using numerical modelling for the nonlinear material behaviour, supported by field observations and measurements performed on several walls, and taking into account the interaction between the soil and wire mesh reinforcements, the parametric study shed more understanding on how the main design parameters, including its limiting height and with to height ratio, influence the overall wall behaviour.

REFERENCES

- Kovári, K. and Amstad, Ch. (1982). Technical note: A new method of measuring deformations in diaphragm walls and piles. *Geotechnique*, 32(4), 402-406.
- Lo, S.-C.R. (1990). Determination of design parameters of a mesh-type soil reinforcement. *Geotechnical Testing Journal*, 13(4), 343-350.
- Stanić, B., Kovačević, M.S., Szavits-Nossan, V. (2001). Deformation and stiffness measurements in reinforced soil. *Proc. XV Internl. Conference on Soil Mechanics and Foundation Engng.*, Istanbul. Balkema, 2, 1257-1260.
- Stanić, B. (2002). *Reinforced earth wall deformations*. PhD Thesis. University of Zagreb, Faculty of Civil Engineering.
- Stanić, B., Kovačević, M.S., Szavits-Nossan, V. (2003). Assessment of deformations of a reinforced soil structure. *Proc. XIIIth European Conference on Soil Mechanics and Geotechnical Engng.*, Prague, Czech Geot. Soc., 2, 887-892.
- Szavits-Nossan, A. and Kovačević, M.S. (1994). A kinematic hardening soil model for wide shear strain ranges. *International Journal for Engineering Modeling*, 7(3-4), 55-63.
- Szavits-Nossan, A., Kovačević, M.S., Szavits-Nossan, V. (1999). Modeling of an anchored diaphragm wall. *Proc. Internl. FLAC Symp. on Numerical Modeling in Geomechanics: FLAC and Numerical Modeling in Geomechanics*. Minneapolis, Balkema, 451-458.